The influence of the geometry and the material properties on the behavior of the human knee

VALERICA MOŞNEGUŢU, VETURIA CHIROIU
LUCIAN CĂPITANU
Institute of Solid Mechanics of Romanian Academy
Ctin Mille 15, P O Box 1-863, Bucharest 010141
valeriam732000@yahoo.com, http://www.imsar.ro

MIHAI POPESCU
The Clinical of Ortopaedics-Traumatology and Osteoarticular TBC Foisor
Ferdinand 35-37, Bucharest 021382
mvpopescu@gmail.com, http://www.foisor.ro

Abstract: - In this paper, the motion of the knee joint during flexion and extension is investigated. It is developed a mathematical model of the knee joint that describes motion in 12 generalized coordinates as a function of the externally motion. The model is based on the patellar track geometry experimental data. The surface of the patellar track is modeled by using the *n*-ellipsoid model. The inverse problem is restricted to slow motions, so we consider that static optimization is good enough for our goal.

Key-Words: knee joint motion, surface modeling, *n*-ellipsoid model, patellar track geometry, geometric and natural compatibilities.

1 Introduction

The knee joint is one of the most complex joints in the human body. The problem of the shape of bones and the position of ligaments with given properties represents the key for evaluation of knee joint properties, and also for study the knee motion. Usually, the tibial plateau and the condyles are modeled by geometric approximations of the bones or by finite element descriptions obtained by computer tomography and magnetic resonance tomography [1]. Also, the points of attachment to the bones simulate the ligaments by using the spring-damper elements between the thigh and the shank [2]. Zheng *et al.* describe an analytical model for ligaments, muscles and contact forces between bones and menisci to examine the joint forces during exercise and restricted to the sagittal plane [2].

Another works model the passive joint motion without load, by using five constraints in terms of three ligaments and the medial and lateral compartment of the knee to model the passive joint movement without load [3],[4]. On the other hand, the surface errors can generate large errors in kinetic and kinematic simulations of articular joint contacts. To avoid such errors, the bone surfaces have to be modeled as highly curved surfaces, with unknown parameters which can be determined from experimental data.

The knee joint surface modeling must verify the geometric and also, the natural compatibility conditions. The geometric compatibility condition assures that the distance between the contact points on the two surfaces is zero, such that the penetration is avoided. The natural compatibility condition assures that normals to the surfaces at the point of contact are collinear. A method based on 2D polynomials to fit bone surface geometry is described in [5]-[8]. Generally, it is observed that small errors can create penetration of the two objects in contact and result in multiple contact points.

Another method which uses polygons to represent bone surfaces is resented in [9]. In this paper, the natural compatibility condition is not necessarily satisfied, and the coplanar, colinearity of normals at the contact point are not verified. Using the cubic splines in investigation of parametric surface patches is investigated in [10]-[16]. Here, errors are possible for points at other locations on a patch which can lead to discontinuous contact points in simulations of joint contact. The use of B-splines to create geometric models of articular surfaces improve the accuracy of this extrapolation grid, but it may not represent highly curved surfaces and it requires that the digitized anatomy be regularly distributed [17].

The present paper investigates the motion of the patella relative to the thigh, by constructing an

inverse problem based on experimental data and simulation of the patellar track geometry as an *n*-ellipsoid model.

Inverse problems have a well-recognized position in research fields, where the values of some model parameters or material properties are obtained from the experimental data. The shape determination, estimation of material properties, experimental strategy, system determination, boundary condition and source identification, defects identification, non-destructive testing and characterization of materials and structures, are examples of inverse problems

The inverse problem reverses the role between the unknowns and the data. When we study a phenomenon, which is governed by a set of equations, the application of the model to real problems requires the knowledge of parameters which in the model are considered to be known whereas, in practice, they are not known. Therefore, a preliminary treatment of the model is necessary, in which parameters are identified from experimental data.

2 Knee anatomy

The important parts of the knee include the end of the femur, the top of the tibia, articular cartilage AC, meniscus cartilage, four ligaments, and two tendons: the anterior cruciate ligament ACL, the posterior cruciate ligament PCL, the medial collateral ligament MCL, the lateral collateral ligament LCL, the quadriceps tendon (QT) and the patellar tendon (PTL) (Fig.1). The apparent space between the bones is actually occupied by articular cartilage AC.

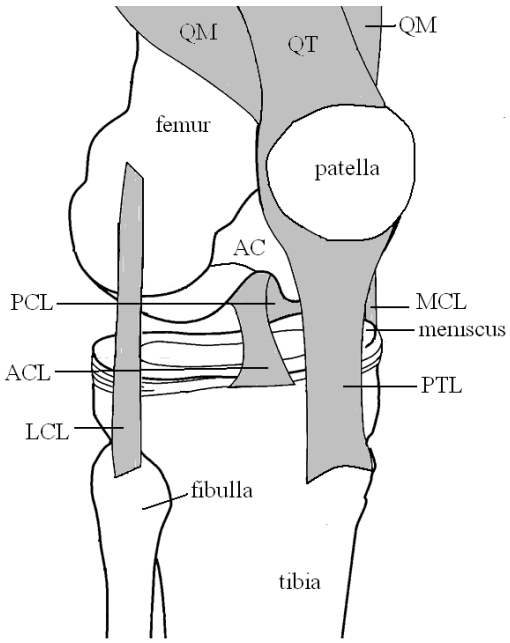

Fig.1. Schematic of the knee muscles and ligaments.

The articular surfaces are the large curved condyles of the femur, the flattened condyles of the tibia, and the facets of the patella. The articular cartilages (AC) act bearing surfaces and the meniscus as mobile bearings.

There are large muscles in the front of the thigh (the quadriceps muscles QM) that straighten the knee (extension). The large muscles in the back of the thigh (the hamstrings) bend the knee (flexion). The patella functions as an important lever for the quadriceps muscles, making the muscle more efficient. When bending and straightening the knee, the surfaces of the tibia and femur roll and slide on each other and the patella moves up and down against the front of the femur. The quadriceps tendon (QT) and the patellar tendon (PTL) surround the patella and helps its mechanical motion and also functions as a cap for the condyles of the femur.

This paper tries to solve the following problem: given the ligaments, tendons and muscle forces, flexion-extension and internal-external rotation angles of the knee, find the motion of the patella relative to the thigh during flexion. The muscle forces and the flexion–extension and internal-external rotation angles of the knee are determined from experimental data of the patellar track geometry. For the patellar geometry an *n*-ellipsoid model is used.

The inverse problems are typically ill-posed in the sense of Hadamard, as opposed to the well-posed problems where the model parameters or material properties are known. This means that the solution of the inverse problem either does not exist, is non-unique, or does not depend continuously in the data.

3 The theory

Position of the knee joint is described by the origin of local coordinate system with respect to global coordinates. The attitude is described by the orientation of local coordinate system with respect to global axes (a local coordinate system is considered for each bone) (Fig.2). So, we have a femoral coordinate system (x_f, y_f, z_f), a tibial coordinate system (x_t, y_t, z_t) and a patellar coordinate system (x_p, y_p, z_p). The origins of the femoral and tibial coordinate systems are located at the midpoint of the line between the medial and lateral femoral epicondyles and the medial lateral tibial condyles, respectively. The origin of the

patellar coordinate system (x_p, y_p, z_p) is located at the centroid of the patella. In all three coordinate systems, the medial x, posterior y, and superior z directions were chosen to be positive and were assumed to be parallel to a global coordinate system (x, y, z). In the global coordinate system, the (x, y) plane was defined as the coronal plane and the (y, z) plane was defined as the sagittal plane.

In the global system, a point belonging to knee joint articular surface Γ is denoted by (x, y, z). In the local coordinate systems, a point belonging to Γ is defined by (x'_L, y'_L, z'_L), where L denotes the local system.

The transformation from (x'_L, y'_L, z'_L) to (x, y, z) is given by

$$x_i = u_i + R_{ik} x'_{kL}, \tag{1}$$

where R_{ij} is the rotation matrix

$$R = R(z,\varphi)R(x,\theta)R(z,\psi),$$

with

$$R(z,\psi) = \begin{bmatrix} \cos\psi & -\sin\psi & 0 \\ \sin\psi & \cos\psi & 0 \\ 0 & 0 & 1 \end{bmatrix},$$

$$R(x,\theta) = \begin{bmatrix} 1 & 0 & 0 \\ 0 & \cos\theta & -\sin\theta \\ 0 & \sin\theta & \cos\theta \end{bmatrix},$$

$$R(z,\varphi) = \begin{bmatrix} \cos\varphi & -\sin\varphi & 0 \\ \sin\varphi & \cos\varphi & 0 \\ 0 & 0 & 1 \end{bmatrix}, \tag{2}$$

and u the translation vector.

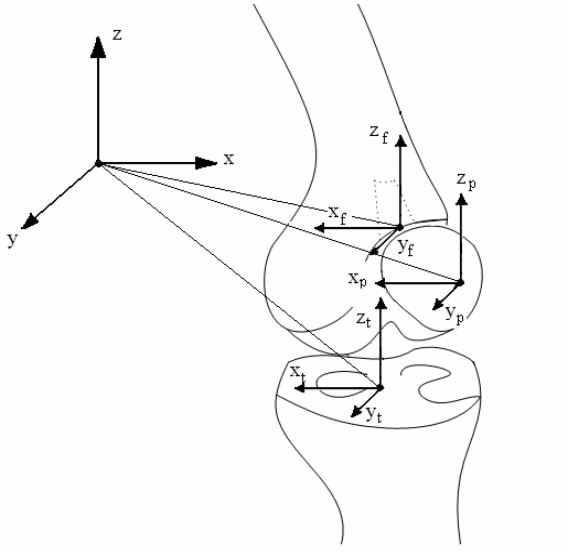

Fig. 2. The global and local systems of coordinates.

We suppose that six generalized coordinates described the movement of the patella relative to the thigh (Fig.3). The patella is treated as a massless body in the model. The orientation of the patella was defined by a sequence of three rotations about the local mutually perpendicular joint axes: patellar rotation, patellar tilt, and flexion-extension. The displacement of the origin of the patellar reference frame relative to the origin of the thigh reference frame was defined by three translations along the three joint axes: anterior-posterior translation, proximal-distal translation, and medial-lateral translation, respectively [19].

The position and orientation of the knee relative to the global coordinate system fixed on the pelvis are described by 12 generalized coordinates: anterior-posterior translation of the shank relative to the thigh q_1, proximal-distal translation of the shank relative to the thigh q_2, medial-lateral translation of the shank relative to the thigh q_3, anterior-posterior translation of the patella relative to the thigh q_4, proximal- distal translation of the patella relative to the thigh q_5, medial-lateral translation of the patella relative to the thigh q_6; varus-valgus rotation[1] of the knee q_7, internal-external rotation of the knee q_8, flexion–extension of the knee q_9, patellar rotation q_{10}, patellar tilt q_{11}, patellar flexion–extension q_{12}.

So, the 12×1 vector $q = \{q_1, q_2, ..., q_{12}\}$ of generalized coordinates describes the configurations of the tibio-femoral joint and patello-femoral joint.

We suppose that the patellar tendon is inextensible and that interpenetration between the boundaries of the patella and the patellar surfaces of the femur can be neglected. These two assumptions define three holonomic constraints for movement of the patella on the femur. These three constraints can be combined with the six force and moment equilibrium equations for the patella to

[1] Varus is a status of medial deviation in the frontal-plane (adduction) of a segment distal to a joint, or to the proximal end of the same segment – occurs at the knee joint. Valgus is a status of lateral deviation in the frontal-plane (abduction) of a segment distal to a joint, or to the proximal end of the same segment, occurs at the proximal femur. The terms adduction, abduction, rotation describe the motion.

yield a set of six non-linear algebraic equations for patello-femoral mechanics

$$p_i(q,F_Q)=0\,,\quad i=1,2,...,6\,, \tag{3}$$

where F_Q is the magnitude of the force applied by the quadriceps tendon to the patella.

The dynamical equations of the knee motion can be written as

$$\begin{aligned} &A(q)\ddot{q}+C(q,\dot{q})+M_m(q)F_m+M_l(q)F_l+\\ &T(q,\dot{q})=0, \end{aligned} \tag{4}$$

where $A(q)$ is the 12×6 mass matrix, $C(q,\dot{q})$ is a 6×1 vector containing the Coriolis and centrifugal forces and torques arising from the motion of the thigh, F_m is a 6×1 vector of forces applied by two muscles (QM, QT), $M_m(q)$ is a 12×6 matrix describing the moment arms of applied muscle forces, F_l is a 6×1 vector containing the forces applied by four ligaments and two tendons, $M_l(q)$ is a 6×12 matrix describing the moment arms of the knee ligament and tendon forces, and $T(q,\dot{q})$ is an 6×1 vector of external torques applied at the joints. Equations (3), (4) define a system of 12 nonlinear differential and algebraic equations in 12 unknowns.

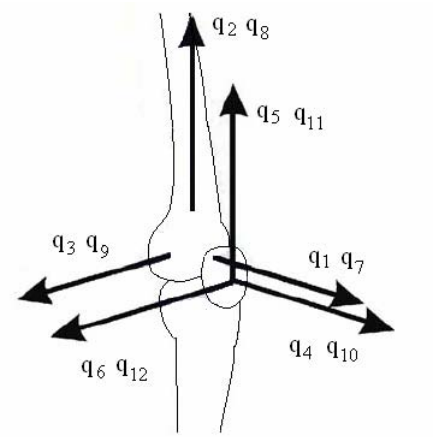

Fig. 3. Kinematic structure of the knee.

The problem to be solved can be stated as:
Given the input data
$I(q,\dot{q})=\{C(q,\dot{q}),T(q,\dot{q}),A(q),M_m(q),\ M_l(q),\ F_m,F_l\}$,
find the motion of the patella relative to the thigh, during flexion.

The main idea of this paper is to determine the unknowns $I(q,\dot{q})$ from the patellar track geometry, based on the experimental data found in literature, for example in [1] and [20].

The method presented in [20] provided an accurate representation of the highly curved surface of the patellar track, and also assures the continuity of the normal vector field.

For determining $I(q,\dot{q})$, we suppose that $C(q,\dot{q})$ and $T(q,\dot{q})$ are expressed as polynomials in q and $\dot{q}$

$$C_j(q,\dot{q})=X_{1j}(q,\dot{q})=\sum_{i=1,12}a_{ij,1}q_i+\sum_{i=1,12}b_{ij,1}\dot{q}_i\,. \tag{5}$$
$$j=1,...,6\,,$$

$$T_j(q,\dot{q})=X_{2j}(q,\dot{q})=\sum_{i=1,12}a_{ij,2}q_i+\sum_{i=1,12}b_{ij,2}\dot{q}_i\,, \tag{6}$$
$$j=1,...,6\,.$$

where a_i, b_i are unknown quantities, and $l=1,2$, $i,j=1,...,k$. For $A(q),M_m(q),\ M_l(q)$ we suppose

$$A_j(q)=Y_{1j}(q)=\sum_{i=1,12}c_{ij,1}q_i,\qquad j=1,...,32, \tag{7}$$

$$M_{mj}(q)=Y_{2j}(q)=\sum_{i=1,12}c_{ij,2}q_i,\quad j=1,...,32, \tag{8}$$

$$M_{lj}(q)=Y_{3j}(q)=\sum_{i=1,12}c_{ij,3}q_i,\quad j=1,...,32, \tag{9}$$

where c_i are unknowns, $s=1,2,3$, $i,j=1,...,k$. The quantities F_m,F are supposed to be constants. The idea is to obtain a reasonable stable simulation model which can handle realistic loads.

For identification problem, the patellar track geometry denoted by Γ is modelled as an *n*-ellipsoid model [21]-[23].

The *n*-ellipsoid is defined by 10 shape parameters d_i, $i=1,2,...10$, that are the arbitrary center coordinates x_G,y_G,z_G, principal axes a,b,c, the principal directions defined by Euler angles ξ,ψ,ζ and the exponent n. The advantage of this model is the small number of parameters needed to represent a surface. The surface Γ is defined as the image of the unit *n*-sphere S of equation

$$x^n+y^n+z^n=1\,, \tag{10}$$

through the affined transformation

$$y=(Y_1,Y_2,Y_3)\in S\rightarrow\ y=(y_1,y_2,y_3)\in\Gamma, \tag{11}$$

$$\begin{aligned} y_1&=x_G+r_{11}aY_1+r_{12}bY_2+r_{13}cY_3,\\ y_2&=y_G+r_{21}aY_1+r_{22}bY_2+r_{23}cY_3,\\ y_3&=z_G+r_{31}aY_1+r_{32}bY_2+r_{33}cY_3, \end{aligned}$$

where $r_{ij}=r_{ij}(\xi,\psi,\zeta)$ are components of rotation,

which transforms the coordinate axes into the principal axes of the ellipsoid. These components are given by (2) by replacing θ with ξ, and φ with ζ. An inverse problem is constructed for finding the set of parameters (shape parameters $d_i, i=1,2,...10$) and unknown model parameters $P_s=\{a_{il},b_{il},....\}$, $s=1,2,...,P$, such that the *n*-ellipsoid best fits the set of data points representing the motion of pattela.

A genetic algorithm is used to solve the identification inverse problem. The estimation of the unknown parameters P_s, $s=1,2,...,P$

$$P_s=\{\, d_j,\ i=1,2,...,10;\ a_{jk,l},b_{jk,l},c_{jm,n},\ j=1,...,12;\ k=1,...,6;\ l=1,2;m=1,...,32;\ n=1,2,3\}, \quad (12)$$

is made for non-perturbed data and artificially perturbed data introduced by multiplication of the data values by $1+r$, r being random numbers uniformly distributed in $[-\varepsilon,\varepsilon]$. In this paper we consider $\varepsilon=10^{-3}$. The algorithm for analysing a surface is as follows:

1. Experimental track the patella surface is used to obtain a high number of 3D contact points in the system of coordinates (x_p,y_p,z_p). M points along the surface are probed, and at each point, two data samples are taken to verify the integrity of the data. Therefore, a total of $3M$ data points are acquired for the surface.

2. Transform the data to $3M$ points (x_i,y_i,z_i), $i=1,...,3M$ belonging to the surface Γ for performing the n-ellipsoid fit.

3. Calculate the set of P parameters that define the motion of the surface Γ such that the n-ellipsoid best fits the set of data points, by using a genetic algorithm.

4. Determine the best approximating shape of the patella during the motion.

4 The genetic algorithm

Optimization methods could be divided into derivative and non-derivative methods. The genetic algorithm is a non-derivative methods, as it is more suitable for engineering design problems. One reason is that non-derivative methods do not require any derivatives of the objective function in order to calculate the optimum.

The principles of natural selection have been formulated by Darwin before the discovery of genetic algorithm. Darwin hypothesized that parental qualities combine together like fluids in the offsprings [24], [25]. This selection theory arose serious objections, that are the crossing fast levels off any hereditary distinctions, and there is no selection in homogeneous populations (*the Jenkins nightmare*).

Genetic algorithms use the vocabulary of the natural genetics. The individuals in a population are called strings or chromosomes. Chromosomes are made of units called genes arranged in linear succession. Every gene controls the inheritance of one or several characters.

The genetic algorithm is able to solve nonlinear, nonlocal optimization problems, without the need of derivative calculations. Starting with a set of initial solutions, the genetic algorithm progressively modify the solution set by mimicking the evolutionary behavior of biological systems, until an acceptable result is achieved.

The genetic algorithm is a binary-coded algorithm, each individual member of the population is represented in binary form. The method is based on an assigning measure of fitness to each individual related to the value of the objective function at the corresponding point in the solution space.

A proper formulation of the optimisation problem is to determine the set of parameters P_s, $s=1,2,...,P$ given by (12), from the condition of minimizing of an objective function f

$$f(P_k)=\sum_{i=1}^{m} w_i \frac{\sum_{j=1}^{N_i}\left|\frac{F_{ij}^t(P_k)-F_{ij}^e(P_k)}{F_{ij}^e}\right|}{N_i}+\sum_{j=1}^{6} w_j S_j^2\ , \quad (13)$$

where $i=1,2,...,m$ represent the number of sequence in the patellar track geometry, F_j^t, $j=1,2,...,3N$, represent the theoretical coordinates of j points belonging to the surface of patella associated to the sequence i, obtained from the theoretical model in terms on P_k, $k=1,2,...,P$, F_j^e are the measured corresponding coordinates of the same j points belonging to the surface of patella associated to the sequence i, and w_i are weights. In (13), s_i, $i=1,2...,6$ represent the measure for verifying (3)

$$s_i=p_i(q,F_Q)\,,\ i=1,2,...,6\,. \quad (14)$$

The basic operators of the genetic algorithm are selection, crossover and mutation. Selection involves the choice of the individuals for the generation of offspring. By using the fitness function (or fitness), a rule for selecting which

individuals to use to create the next generation must be chosen.

Crossover is the method of combining two individuals to produce an offspring. The proportion of a population that is mated after each generation is defined by the cross-over rate. The experiments performed suggested an optimum tuning of the cross-over rate is 0.8.

Mutation is the random changing of some individual within the population. A flow chart of the genetic algorithm can be presented as:

{
*** Initialisation of time contor
$t := 0;$
*** population random initialisation
initpopulation $P(t);$
***evaluation of the fitness for all individuals
evaluate $P(t);$
*** stop test
while not done do
*** increase the time contor
$t := t + 1;$
*** selection of a subpopulation to produce offspring
$P' :=$ selectparents $P(t);$
*** recombination of genes of chosen parents
recombine $P'(t);$
*** apply mutation to each offspring
mutate $P'(t);$
*** evaluation of the new fitness function
evaluate $P'(t);$
*** selection of individuals according to the fitness function value
$P :=$ survive $P, P'(t);$
}.

The genetic algorithm uses a binary vector as a chromosone to represent real values of the variable x. The length of the vector depends on the required precision. The domain of of the variable $x \in [a,b]$ has length $l = b - a$ and the precision requirement implies that the range of the interval should divided into at least $l \times 10^6$ equal size ranges.

Now we need to solve the inverse problem: first compute a displacement field δX between the n-ellipsoid and $3M$ point data, and then, after having put the n-ellipsoid in a 3D box, search for the "deformation" δP of this box which will best minimize the displacement field δX

$$J(\Gamma) = \min_{\delta P} \| B\delta P - \delta X \|^2 \ . \tag{15}$$

In other words Γ is classically sought as the minimizer of some distance $J(\Gamma)$ between the measured data and the computed n-ellipsoid data.

To represent 3D data with our model, we use an iterative two-step algorithm:

Step 1: Computation of the displacement field between the previous estimation X_n and its projection on data X_n^a, δX_n such as

$$X_n^a = X_n + \delta X_n . \tag{16}$$

Step 2: Computation of the control points P_{n+1} by minimization of $\| BP - X_n^a \|^2$ and computation of the deformed model

$$X_{n+1} = BP_{n+1} . \tag{17}$$

Stop test on the least-squares error $\| X_{n+1} - X_n \|$. The quantity P_0 is defined as a uniformly spaced parallelepiped box of control points and $X_0 = BP_0$ represents the set of points of the initial discretized n-ellipsoid.

Because the same n-ellipsoid can result from many combinations of angles ξ, ψ and ζ and permutations of principal axes, it is difficult to measure the accuracy of the identification of Γ. The optimization methods used in optimal control is based on a proper identification of Γ [25], [26], [30]. The accuracy may be measured by means of comparison of the identified parameters P_k, $k = 1, 2, ..., P$ with those defining the true Γ and used to compute the simulated data. Instead of this, the relative errors $\varepsilon_V, \varepsilon_A, \varepsilon_I$ for the volume, boundary area and geometrical inertia tensor (with respect to the global system of coordinates (x, y, z)) are computed.

The indicator ε_I is very sensitive to the orientation of Γ in space, together with the ratio J_n / J_0, where $J_n = J(\Gamma_n)$ and Γ_n is the current Γ after the n-th iteration of the minimization process. Expressions of indicators $\varepsilon_V, \varepsilon_A, \varepsilon_I$ in terms of boundary integrals are as follows [27]-[29]

$$\varepsilon_V = \frac{V(\Gamma_n)}{V(\Gamma)} - 1, \quad V(S) = \frac{1}{3}\int_S y_i n_i \mathrm{d}S_y , \tag{18}$$

$$\varepsilon_A = \frac{A(\Gamma_n)}{A(\Gamma)} - 1, \quad A(S) = \int_S \mathrm{d}S_y , \tag{19}$$

$$\varepsilon_I = \left(\frac{\sum_{1 \le i,j \le 3} (I_{ij}(\Gamma_n) - I_{ij}(\Gamma))^2}{\sum_{1 \le i,j \le 3} I_{ij}^2(\Gamma)} \right)^{1/2} ,$$

$$I_{ij}(S)=\frac{1}{5}\int_S y_i y_j y_k n_k \mathrm{d}S_y \ . \qquad (20)$$

5 Results

The knee joint flexion is considered next. From experiments it results that the knee offers a relatively small resistance as it flexes from full extension to 90^0.

The ligaments are modeled as elastic elements. The articular cartilage is considered homogeneous isotropic with elastic modulus of 12MPa and Poisson's ratio of 0.45. The menisci are assumed isotropic with 10MPa for **e**lastic modulus and 0.45 for Poisson's ratio. The total initial cross-sectional areas are 42, 60, 18 and 25 mm^2 for the ACL, PCL, LCL and MCL, respectively [24], [28], [30].

The run-time parameters of genetic algorithm are: population size 120, number of generations 100, overall crossover probability 0.9, mutation probability 0.03. The number of iteration for finding the parameters P_k, $k=1,2,...,P$ such that the *n*-ellipsoid best fits the set of data points. is 509 for non-perturbed data and 612 for perturbed data..

The values of J_{final}/J_0, $\varepsilon_V, \varepsilon_A, \varepsilon_I$ given by (18)-(20) and the least square error $\| BP-X \|$ are displayed in table 1, in the case of non-perturbed data ($\varepsilon=0$) and perturbed data ($\varepsilon=10^{-3}$). Results show a good convergence and accuracy.

Table 1. Results for non-perturbed data ($\varepsilon=0$).

	$\| BP-X \|$	J_{fin}/J_0 10^{-7}	ε_V 10^{-7}	ε_A 10^{-6}	ε_I 10^{-5}
$\varepsilon=0$	1.4 %	3.8	8.3	10.2	9.4
$\varepsilon=10^{-3}$	8.3 %	2.4	3.3	2.3	3.6

The results of the inverse problem are shown in figs. 4, 5 and 6. The upper shape of the surface Γ with $n=0.37$, during flexion is displayed in fig. 4.

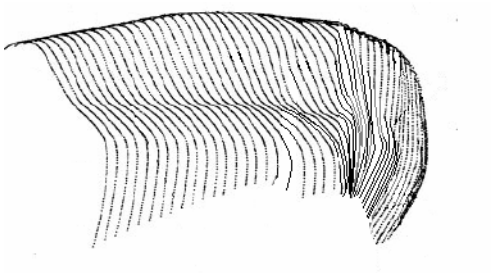

Fig. 4. A sequence of shapes for surface Γ ($n=0.37$) during flexion.

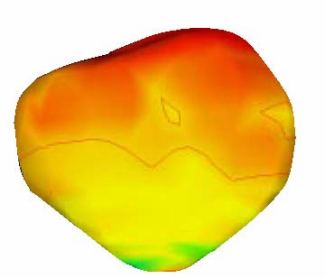

Fig. 5. The shape of patella for Γ ($n=0.37$).

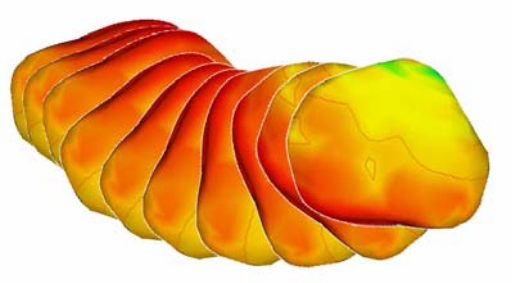

Fig. 6. A sequence of pattela shapes during flexion.

The coefficients $a_{ij,1}$, $a_{ij,2}$, $b_{ij,1}$ and $b_{ij,2}$ that appear in (5) and (6) are shown in appendix (tables A1-A4). Also we have obtained

$$F_l=(13,44;12,86;11,56;10,65;10,07;10,44\},$$
$$F_m=\{2,67;2,26;2,10;1,98;1,67;2,03\}.$$

The lack of space is the reason we do not diplay here the values of the coefficients $c_{ij,1}$, $c_{ij,2}$ and $c_{ij,3}$ that appear in (7)-(9).

During flexion, the patella glides smoothly in this groove throughout an arc of motion (0^0-90^0). The patella trajectory is 4mm deeper. The experimental results (Any Body Technology [32]) are summarized in figs.7 and 8.

Fig. 9 represents the forces in ligaments and tendons during flexion. Forces transmitted to ACL, PCL, MCL, LCL and PTL are plotted versus the flexion angle. The optimization procedure is statically, so the motion and forces may be a little altered, but the optimization method is stable and

works. The PTL and ACL exhibit peaks at 54.25^0 and respectively, 68^0. The MCL have the smallest forces, the LCL exhibits a peak at 73.5^0 and PCL exhibits a peak at 82.5^0.

The translation degrees of freedom, i.e. q_1, proximal-distal translation of the shank relative to the thigh q_2, medial-lateral translation of the shank relative to the thigh q_3, anterior-posterior translation of the patella relative to the thigh q_4, proximal-distal translation of the patella relative to the thigh q_5, medial-lateral translation of the patella relative to the thigh q_6 during flexion are displayed in fig.10. The variation of all translation degrees of freedom (with exception of q_2) are increased functions with respect to the flexion angle. The q_2 begins to decrease in the vicinity of 78.75^0, and near 45^0 it seems to be almost constant.

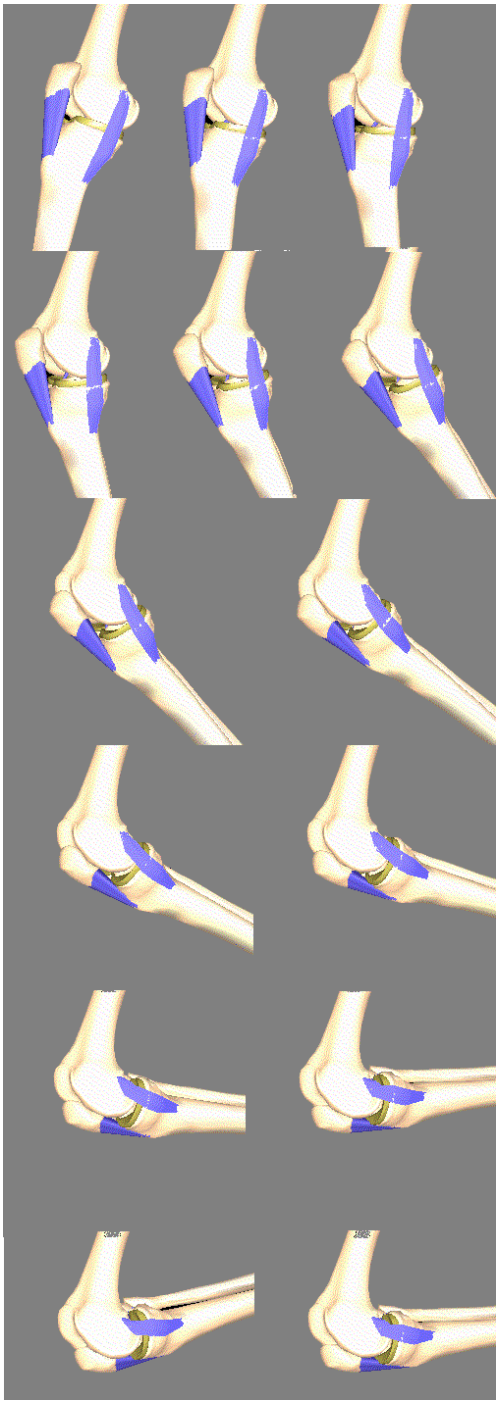

Fig.7. Snapshots of the patella motion [25].

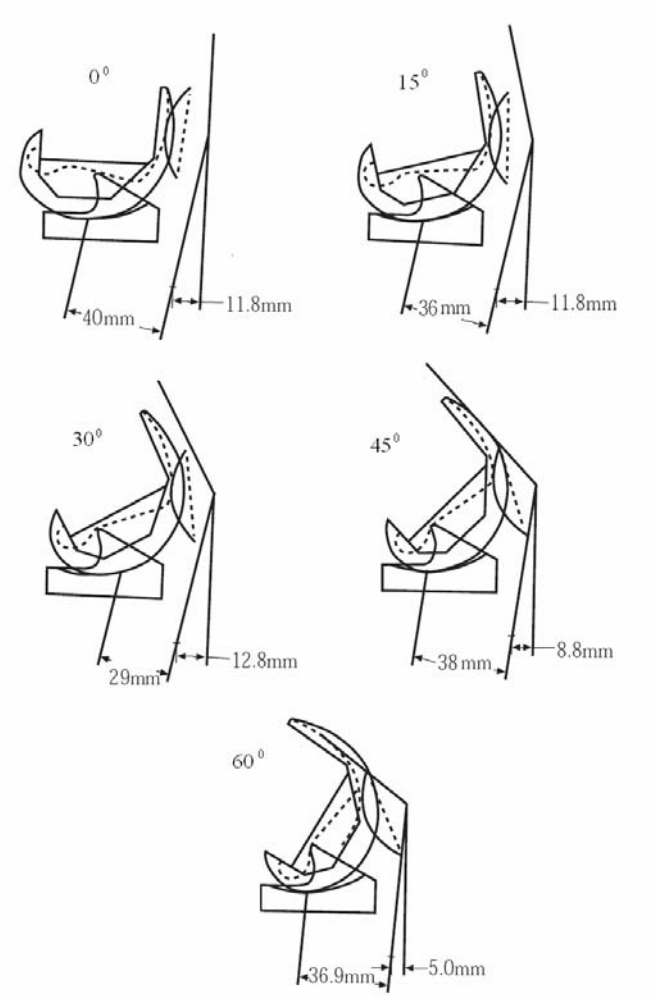

Fig. 8. The position of the patella in relation to the tubercle.

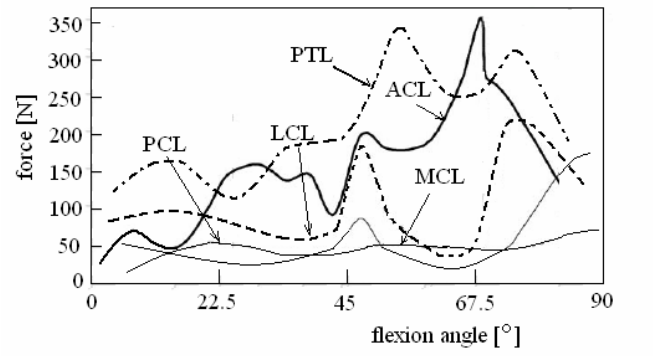

Fig. 9. The forces in ligaments and tendons during flexion.

Fig. 11 presents the rotation degrees of freedom, i.e. varus-valgus rotation of the knee q_7, internal-external rotation of the knee q_8, flexion–extension of the knee q_9, patellar rotation q_{10}, patellar tilt q_{11}, patellar flexion–extension q_{12} during flexion. The variation of q_7 and q_{10} are increased functions with respect to the flexion angle. The other degrees of freedom exhibit increasing and decreasing regions with respect to the flexion angle.

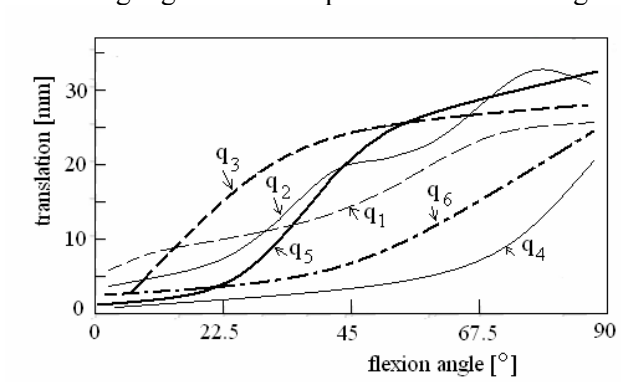

Fig. 10. The translation degrees of freedom during flexion.

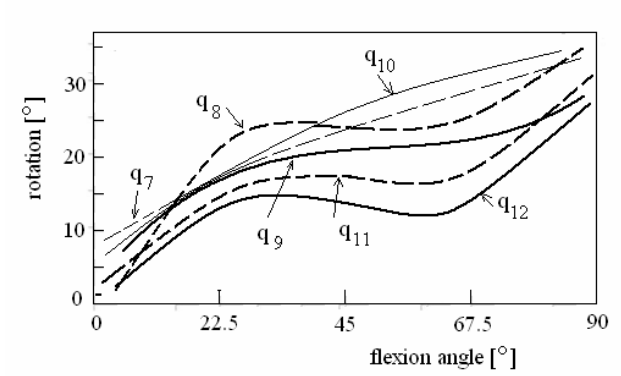

Fig. 11. The rotation degrees of freedom during flexion.

The similar figures in the case of extension are presented in figs.12, 13 and 14.

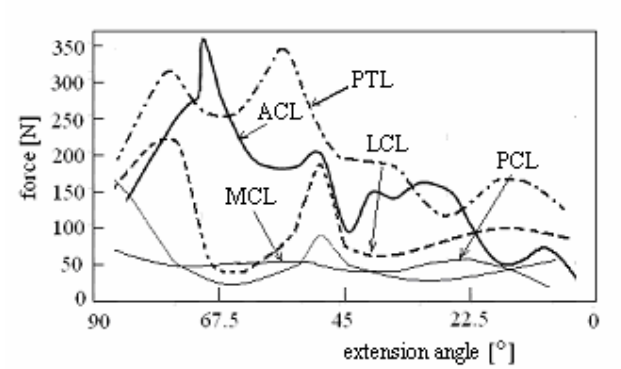

Fig. 12. The forces in ligaments and tendons during extension.

The knee motion is the result of the full-body movement, so it is difficult to model only the knee motion without taking into consideration the body influences. For this reason, the position and orientation of the knee relative to the global coordinate system fixed on the pelvis are described by minimum 12 generalized coordinates.

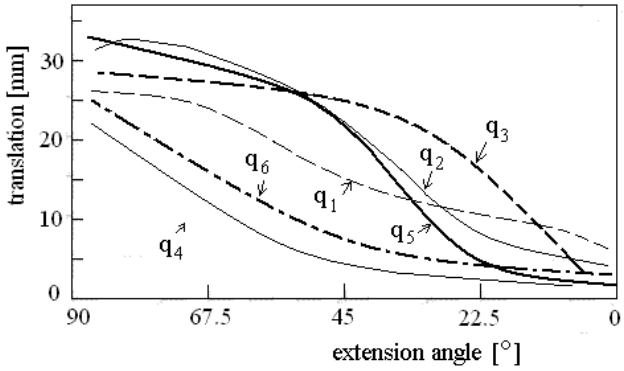

Fig. 13. The translation degrees of freedom during extension.

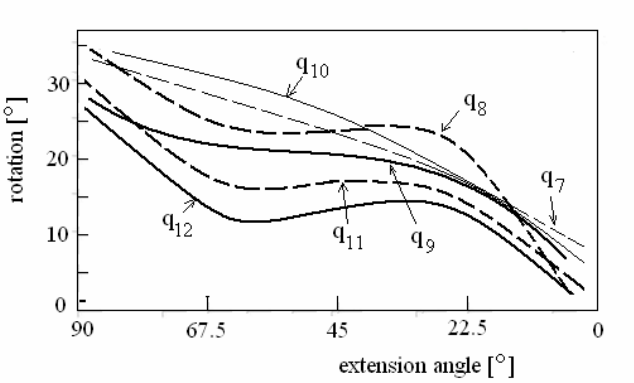

Fig. 14. The rotation degrees of freedom during extension.

6 Conclusions

In this paper, a mathematical model of the knee joint that describes motion in 12 generalized coordinates as a function of the externally load is developed. The model is based on the patellar track geometry experimental data and it is able to describe the motion of the knee joint during flexion and extension.

The surface Γ of the patellar track is modeled by using the *n*-ellipsoid model, defined by 10 shape parameters. The relative small number of parameters needed to represent a surface represent an important advantage of this model. The method is restricted to slow motions, so we consider that static optimization is good enough for our goal.

The motion equations (3), (4) define a system of 12 nonlinear differential and algebraic equations in 12 unknowns. The unknown are the anterior-posterior translation of the shank relative to the thigh q_1, proximal-distal translation of the shank relative to the thigh q_2, medial-lateral translation of the shank relative to the thigh q_3, anterior-posterior translation of the patella relative to the thigh q_4, proximal- distal translation of the patella relative to the thigh q_5, medial-lateral translation of the patella relative to the thigh q_6; varus-valgus rotation[2] of the knee q_7, internal-external rotation of the knee q_8, flexion–extension of the knee q_9, patellar rotation q_{10}, patellar tilt q_{11}, patellar flexion–extension q_{12}.

To solve this system of equations, we need to know some input data. The input data is composed of the Coriolis and centrifugal forces and torques arising from the motion of the thigh $C(q,\dot{q})$, the external torques applied at the joints $T(q,\dot{q})$, the mass matrix $A(q)$, the moment arms of applied muscle forces mass matrix $M_m(q)$, the moment arms of the knee ligament and tendon forces $M_l(q)$, the forces applied by two muscles (QM, QT) F_m, and the forces applied by four ligaments and two tendons F_l. The input data is determined from the patellar track geometry, based on the experimental data found in literature

The inverse problem is constructed in such a way to evaluate simultaneously the set of unknown parameters from the condition that the *n*-ellipsoid best fits the set of experimental data points.

The approach is restricted to slow knee motions, and the static optimization based ob a genetic algorithm is used to determine the unknowns.

The inverse problems is ill-posed and have to be overcome by developments of new computational methods. The traditionally local optimisation methods based on the matrix inversion, steepest descent and conjugate gradients are trapping into local minima and their success depends on the choice of starting conditions. To obtain further insights into the inverse problems related to the identification of certain parameters or to solve some nonlinear equations, the genetic algorithm is used. Genetic algorithm is a search method suitable for the global optimization of multi-objective functions. Starting with a set of initial solutions, this algorithm progressively modifies the solution by mimicking the evolutionary behavior of biological systems, until an acceptable result is achieved.

[2] Varus is a status of medial deviation in the frontal-plane (adduction) of a segment distal to a joint, or to the proximal end of the same segment – occurs at the knee joint. Valgus is a status of lateral deviation in the frontal-plane (abduction) of a segment distal to a joint, or to the proximal end of the same segment, occurs at the proximal femur. The terms adduction, abduction, rotation describe the motion.

An easy way to verify the results is to solve the direct approach, by using the input data identified by the inverse problem.

In conclusion, the model considered in the paper is reasonable stable and can handle realistic results.

Appendix.

Table A1. The coefficients $a_{ij,1}$.

a11.1	0.54	a12.1	-0.04	a13.1	-0.04
a21.1	0.32	a22.1	-0.12	a23.1	-0.12
a31.1	-4.21	a32.1	3.27	a33.1	2.22
a41.1	-0.55	a42.1	0.05	a43.1	0.15
a51.1	1.94	a52.1	-1.04	a53.1	-3.64
a61.1	0.53	a62.1	-0.13	a63.1	-0.73
a71.1	0.30	a72.1	0.23	a73.1	0.56
a81.1	-1.10	a82.1	1.23	a83.1	-1.09
a91.1	-2.89	a92.1	3.11	a93.1	-1.88
a10.1.1	4.31	a10.2.1	0.31	a10.3.1	-0.89
a11.1.1	4.12	a11.2.1	-0.42	a11.3.1	-1.52
a12.1.1	0.45	a12.2.1	-0.05	a12.3.1	-2.35

a14.1	2.09	a15.1	-0.44	a16.1	-0.14
a24.1	4.44	a25.1	-1.24	a26.1	-112
a34.1	-1.27	a35.1	-2.27	a36.1	2.71
a44.1	-0.75	a45.1	0.75	a46.1	0.75
a54.1	4.34	a55.1	-1.44	a56.1	-0.07
a64.1	0.43	a65.1	-0.83	a66.1	0.53
a74.1	-0.93	a75.1	-0.34	a76.1	0.25
a84.1	-1.03	a85.1	1.19	a86.1	0.43
a94.1	-3.38	a95.1	1.19	a96.1	2.91
a10.4.1	0.41	a10.5.1	-2.39	a10.6.1	-0.45
a11.4.1	-4.02	a11.5.1	-3.02	a11.6.1	-2.02

Table A2. The coefficients $a_{ij,2}$.

a11.2	-1.15	a12.2	-0.14	a13.2	0.74
a21.2	2.23	a22.2	-0.02	a23.2	1.12
a31.2	-3.22	a32.2	3.07	a33.2	-2.02
a41.2	0.45	a42.2	0.25	a43.2	-0.05
a51.2	-1.95	a52.2	-1.03	a53.2	-3.04
a61.2	-0.03	a62.2	-1.15	a63.2	-0.27
a71.2	0.37	a72.2	2.23	a73.2	-0.95
a81.2	-1.13	a82.2	-1.03	a83.2	-1.19
a91.2	-2.05	a92.2	-3.01	a93.2	-1.08
a10.1.2	4.22	a10.2.2	-1.31	a10.3.2	-0.80
a11.1.2	-3.02	a11.2.2	1.04	a11.3.2	-1.50
a12.1.2	0.05	a12.2.2	1.05	a12.3.2	-2.33

a14.2	2.49	a15.2	0.14	a16.2	0.04
a24.2	4.34	a25.2	-0.44	a26.2	-3.16
a34.2	-1.57	a35.2	-1.77	a36.2	2.71
a44.2	1.75	a45.2	0.70	a46.2	3.75
a54.2	4.30	a55.2	0.40	a56.2	-3.27
a64.2	0.40	a65.2	-0.63	a66.2	0.54
a74.2	-1.43	a75.2	0.64	a76.2	-0.55
a84.2	1.83	a85.2	-1.29	a86.2	-0.73
a94.2	-1.35	a95.1	1.09	a96.1	-2.91
a10.4.2	1.41	a10.5.1	-2.39	a10.6.1	0.45
a11.4.2	4.42	a11.5.1	-3.02	a11.6.1	2.42
a12.4.2	-1.05	a12.5.1	-1.15	a12.6.1	1.25

Table A3. The coefficients $b_{ij,1}$.

b11.1	-0.22	b12.1	1.14	b13.1	1.04
b21.1	-0.39	b22.1	-0.82	b23.1	-0.21
b31.1	-4.21	b32.1	032	b33.1	-4.02
b41.1	-0.55	b42.1	-0.95	b43.1	-4.15
b51.1	1.97	b52.1	-0.33	b53.1	-0.04
b61.1	-0.33	b62.2	0.83	b63.1	-3.73
b71.1	-0.89	b72.2	-0.27	b73.1	3.06
b81.1	-1.00	b82.2	-1.03	b83.1	-1.59
b91.1	-1.09	b92.2	-0.91	b93.1	-1.58
b10.1.1	-0.35	b10.2.2	-0.81	b10.3.1	-0.85
b11.1.1	-0.35	b11.2.2	-2.32	b11.3.1	-1.44
b12.1.1	0.15	b12.2.2	-2.05	b12.3.1	-2.85

b14.1	-3.23	b15.1	1.54	b16.1	-0.94
b24.1	1.04	b25.1	-0.34	b26.1	-0.12
b34.1	2.07	b35.1	2.29	b36.1	-2.78
b44.1	1.05	b45.1	-0.88	b46.1	0.65
b54.1	-4.01	b55.1	-1.64	b56.1	-0.27
b64.2	0.24	b65.1	-0.34	b66.1	0.53
b74.2	0.49	b75.1	-0.78	b76.1	-0.45
b84.2	-1.83	b85.1	1.09	b86.1	0.73
b94.2	-3.08	b95.1	1.17	b96.1	2.91
b10.4.2	0.01	b10.5.1	-2.09	b10.6.1	1.15
b11.4.2	-0.02	b11.5.1	-3.12	b11.6.1	-4.22
b12.4.2	-1.05	a12.5.1	-0.55	a12.6.1	-1.05

Table A4. The coefficients $b_{ij,2}$.

b11.2	0.39	b12.2	1.88	b13.2	1.15
b21.2	2.09	b22.2	-0.34	b23.2	-0.43
b31.2	-2.20	b32.2	0.98	b33.2	-4.44
b41.2	1.15	b42.2	-0.56	b43.2	-1.12
b51.2	-1.90	b52.2	1.34	b53.2	0.65
b61.2	2.32	b62.2	2.23	b63.2	-1.13
b71.2	-0.80	b72.2	0.77	b73.2	3.98
b81.2	-1.45	b82.2	2.34	b83.2	-1.76
b91.2	-1.24	b92.2	2.93	b93.2	-1.05
b10.1.2	-0.29	b10.2.2	-0.75	b10.3.2	-0.93
b11.1.2	-0.98	b11.2.2	-2.23	b11.3.2	-2.92
b12.1.2	0.35	b12.2.2	-2.65	b12.3.2	2.76

b14.2	-0.27	b15.2	-1.12	b16.2	0.88
b24.2	-1.34	b25.2	55	b26.2	0.34
b34.2	2.17	b35.2	2.78	b36.2	-2.85
b44.2	-1.15	b45.2	-0.28	b46.2	-0.23
b54.2	-2.12	b55.2	1.62	b56.2	-3.07
b64.2	0.22	b65.2	-1.38	b66.2	-0.53
b74.2	0.45	b75.2	1.04	b76.2	-0.45
b84.2	-2.13	b85.2	1.08	b86.2	0.03
b94.2	0.08	b95.2	-1.67	b96.2	-2.01
b10.4.2	-0.14	b10.5.2	-2.19	b10.6.2	1.75
b11.4.2	-0.45	b11.5.2	-1.02	b11.6.2	0.72
b12.4.2	0.05	a12.5.2	0.15	a12.6.2	1.35

ACKNOWLEDGEMENT. The authors acknowledge the financial support of the PNII TD project nr. 120/2007, code ID_138/2007.

References:

[1] Frey, M., Riener, R., Michas, C., Regenfelder, F., Burgkart, R., Elastic properties of an intact and ACL-ruptured knee joint: Measurement, mathematical modelling, and haptic rendering, *J. of Biomechanics*, 39, 1371–1382, 2006.

[2] Zheng, N., Fleisig, G.S., Escamilla, R.F., Barrentine, S.W., 1998. An analytical model of

the knee for estimation of internal forces during exercise*, J. of Biomechanics*, 31, 963–967, 1998.
[3] Wilson, D.R., Feikes, J.D., O'Conner, J.J., 1998. Ligaments and articular contact guide passive knee flexion. *J. of Biomechanics*, 31, 1127–1136, 1998.
[4] Feikes, J.D., O'Conner, J.J., Zavatsky, A.B., 2000. A constraint-based approach to modelling the mobility of the human knee joint, *J. of Biomechanics,* 36, 125–129, 2000.
[5] Wismans, J., Veldpaus, F., Janssen, J., Huson, A., Struben, P., A three-dimensional mathematical model of the knee-joint, *J. of Biomechanics*, 13, 677–685, 1980.
[6] Engin, A.E., Moeinzadeh, M.H., *Modeling of human joint structure*, AFAMRL Report, AFAMRL-TR-81-117, 1982.
[7] Blankvoort, L., Kuiper, J.H., Huiskes, R., Grootenboer, H.J., Articular contact in a three-dimensional model of the knee. *J. of Biomechanics* 24, 1019–1031, 1991.
[8] Tumer, S.T., Engin, A.E., Three-Body segment dynamic model of the human knee. *J. of Biomechanical Engineering ASME Transactions,* 115, 350–356, 1993.
[9] Delp, S.L., Loan, J.P., A graphic-based software system to develop and analyze models of musculoskeletal structures. *Computers in Biology and Medicine*, 25, 21–34, 1995.
[10] Ateshian, G.A., Soslowsky, L.J., Mow, V.C., Quantitation of articular surface topography and cartilage thickness in knee joints using strereophotogrammetry, *J. of Biomechanics,* 24, 761–776, 1991.
[11] Hirokawa, S., Three-dimensional mathematical model analysis of the patellofemoral joint, *J. of Biomechanics,* 24, 659–671, 1991.
[12] Scherrer, P.K., Hillberry, B.M., Piecewise mathematical representation of articular surfaces, *J. of Biomechanics*, 12, 301-311, 1979.
[13] Scherrer, P.K., *Determining the distance between the surface of two rigid bodies using parametric surface patches and an instrumental spatial linkage*, thesis, Purdue Univ., 1977.
[14] Hart, W.B., Computer graphics aid fuselage design. The leastsquares, *Engineering Materials and Design Institute*, 205–209, 1974.
[15] Almond, D.B., Numerical control for machining complex surfaces, *IBM Systems Journal*, 150–168, 1991.
[16] Hefzy, M.S., Yang, H., A three-dimensional anatomical model of the human patellofemoral joint, for the determination of the patello-femoral motion and contact characteristics, *J. of Biomechanical Engineering*, 15, 289–302, 1993.
[17] Ateshian, G.A., A B-spline least-squares surface-fitting method for articular surfaces of diarthrodial joints, *J. of Biomechanical Engineering* 115, 366-373, 1993.
[18] Mensch, J.S., Amstutz, H.C., *Knee morphology as a guide to knee replacement*, Clinical Orthopaedics 112, 231–241, 1975.
[19] Shelburne, K.B., Pandy, M.G., Anderson, F.C., Torry, M.R., Pattern of anterior cruciate ligament force in normal walking, *J. of Biomechanics*, 37, 797–805, 2004.
[20] Dhaher, Y.Y., Delp, S.L., Rymer, W.Z., The use of basis functions in modelling joint articular surfaces: application to the knee joint, *J. of Biomechanics,* 33, 2000, 901–907.
[21] Bonnet, M., *Shape identification problems using boundary elements and shape differentiation*, Proc. of the 2-nd Conf. on Boundary and Finite Element, 35–48, 1993.
[22] Chiroiu, V., Munteanu, L., Nicolescu, C.M., *Shape description of general 3D object using tactile sensing information,* AMSE: Advances in Modelling, Series B: Signal Processing and Pattern Recognition, 47, 3, 81–90, 2004.
[23] Chiroiu, V., *Identification and inverse problems related to material properties and behavior*, Topics in Applied Mechanics**,** Ed.Academiei, Bucharest, 2003, chapter 4.
[24] Goldberg, D.E., *Genetic algorithms in search, optimization, and machine learning*, Massachusetts: Addison-Wesley Publishing Co., 1989
[25] Chryssoverghi I., Discretization-Optimization Methods for Optimal Control Problems, *WSEAS Transactions of Mathematics*, Vol.4, No.3, 125-132 , 2005.
[26] Itoh, T., Algebraic Geometrical Treatment of Numerical Algorithms, *WSEAS Transactions of Mthematics*, Vol.2, No.1 and 2, 13-20, 2003.
[27] Bonnet, M., Shape identification problems using boundary elements and shape differentiation, *Proc. of the 2-nd National Conf. on Boundary and Finite Element*, ELFIN2, Sibiu, 35–48, 1993.
[28] Chiroiu, V., Munteanu, L., Nicolescu, C.M., Shape description of general 3D object using tactilesensing information*, AMSE: Advances in Modelling, Series B: Signal Processing and Pattern Recognition*, 2003.
[29] Moglo, K.E., Shirazi-Adl, A., Cruciate coupling and screw-home mechanism in passive knee joint during extension–flexion*, J. of Biomechanics* 38, 1075–1083, 2005.
[30] V.Mosnegutu, M.Popescu, V.Chiroiu, L.Capitanu, On the dynamic model of the human

knee, *9th WSEAS International Conference on Acoustics & Music: Theory & Applications* (AMTA '08) http://www.worldses.org/files/romania2008.pdfBuch arest, Romania, June 24-26, Springer, 2008

[31] Purcaru, D., Niculescu. E., Contributions to Shape Description and Model Classification, *WSEAS Transactions of Mathematics*, Vol.5, No.5, 479-485 , 2006.

[32] Any Body Technology
http://www.anybodytech.com/